Iranian Journal of Medical physics
Vol. 8, No. 1, Winter 2012, 9-17
Received: January 16, 2012; Accepted: February 01, 2012

Original Article

Introducing an Optimized Method for Obtaining X-ray Diffraction Patterns of Biological Tissues

Ali Chaparian[1*], Mohammad Ali Oghabian[2], Vahid Changizi[3]

Abstract

Introduction
Individual X-Ray diffraction patterns of biological tissues are obtained via interference of coherent scattering with their electrons. Many scientists have distinguished normal and cancerous breast tissue, bone density, and urinary stone types using the X-Ray diffraction patterns resulting from coherent scattering. The goal of this study was to introduce an optimized method for obtaining X-ray diffraction patterns of different types from biological tissues.

Materials and Methods
A special tool constituting primary and scatter collimators as well as a sample holder was designed and built. All measurements were done using an X-ray tube, the above-mentioned tool, and a semiconductor detector (HPGe). The X-ray diffraction patterns of some tissue-equivalent materials (acrylic, polyethylene, nylon, and calcium carbonate) and biological tissues (adipose, muscle, and bone) were obtained.

Results
The corresponding peak positions for adipose, muscle, bone, acrylic, polyethylene, nylon, and calcium carbonate in corresponding X-ray diffraction patterns are located in 1.1±0.055 nm^{-1}, 1.41±0.072, 1.6±0.08 nm^{-1}, 0.8±0.04 nm^{-1}, 1.03±0.051 nm^{-1}, 1.22±0.061 nm^{-1}, and 1.7 ± 0.085 nm^{-1}, respectively.

Discussion and Conclusion
The X-ray diffraction patterns obtained in this study were in good agreement relative to previous measurements in terms of peak position. This study introduces a useful setup for extraction of X-ray diffraction patterns from different biological tissues.

Keywords: Biological Tissues, Coherent Scattering, X-Ray Diffraction

1- Medical Physic Dept., Shahid Sadoughi University of Medical Sciences, Yazd, Iran
*Corresponding author: Tel: +98 351 8203410-7; Fax: +98 351 8202632; email: chaparian@ssu.ac.ir
2- Medical Physic Dept., Tehran University of Medical Sciences, Tehran, Iran
3- Radiology Technology Dept., Tehran University of Medical Sciences, Tehran, Iran

1. Introduction

In recent years, new techniques have emerged that use coherently scattered photons as a diagnostic method. The X-ray diffraction pattern is obtained for each tissue using interference of these photons with electrons of materials. These X-ray diffraction patterns are unique signatures of the tissues and therefore can be used to characterise them. The X-ray diffraction patterns are usually expressed as a function of momentum transfer (χ) in terms of nanometer (nm^{-1}):

$$\chi = (E/hc).\sin(\theta/2) \quad (1)$$

where E is the photon energy, h is Planck's constant, c is the speed of light, and θ is the scattering angle. There are two basic methods for extracting X-ray diffraction patterns from tissues including angular dispersive X-ray diffraction (ADXRD) and energy dispersive X-ray diffraction (EDXRD). In ADXRD, the diffraction pattern is obtained using monoenergetic photons and recording the angular distribution of scattered photons. This method is performed by a laboratory powder diffractometer or in synchrotron centers so their clinical application is impossible. Alternatively, EDXRD is based on using a polyenergetic photon spectrum obtained from a conventional X-ray tube. In such a system, scatter intensity is recorded at a fixed scatter angle by an energy-resolving detector (e.g. HPGe). Unlike the first method, this method is potentially suitable for clinical usage [1].

A number of authors have used the coherently scattered photons for distinguishing normal from cancerous breast tissue, various kidney stone types, and different bone constituents [2-5]. For example, the X-ray mammography is the gold standard test for screening but it can't differentiate between normal fibrosis and adenocarcinomatous tissues whereas these tissues can be distinguished using their unique scatter signatures.

Kidane et al. obtained X-ray diffraction patterns from breast tissue using EDXRD. A 2.5 mm Al filtered 80 kVp beam (tungsten anode, 10 mA) was collimated so that the scattering volume had dimensions of 4.8 mm length, 0.25 mm width, and 20 mm height. The measurements were performed in scatter angle of 6°. They concluded that these tissue scatter signatures could enhance contrast in mammography [6].

Poletti et al. used a powdered diffractometer operating in ADXRD method to measure the coherently scattered photons for breast tissue. The breast tissue samples were packed in 8 mm diameter acrylic cylindrical containers with 0.1 mm thick walls. A NaI (Tl) detector was used to record the scattered photons at angles between 1.3° and 72° ($0.2\ nm^{-1} < x < 8.3\ nm^{-1}$) in 1/3° increments. Their study focused on measuring the X-ray diffraction patterns generated by normal breast tissue and tissue equivalent phantoms (PMMA, nylon, and polyethylene). Their goal was to understand the characteristics of the low angle scattered field so that better systems (e.g., grid) could be planned to reduce them in conventional mammography procedures [7].

Changizi et al. employed EDXRD using a conventional X-ray tube and a semiconductor detector for normal breast tissue characterization. The measurement time for each sample was 500-600 seconds [8, 9].

LeClair et al. used EDXRD-based measurements coupled with a semianalytical model to extract the X-ray diffraction patterns from breast tissue. This technique was validated using a 50 kV polychromatic X-ray beam incident on a sample of water. Water was used because good X-ray diffraction data were already available in the literature. The scatter profiles were measured using a cadmium zinc telluride detector and the duration of each measurement was 600 seconds. The averages of their results compared well with the golden standard data [10]. An average 7.68% difference for which most of the discrepancies could be attributed to the background noise at low angles was obtained. Their preliminary measurements attained from breast tissue were also encouraging [2].

Ryan et al. utilized two radiation scatter interactions in order to differentiate malignant

from non-malignant breast tissue. These two interactions were Compton scatter, used for measuring the electron density of the tissues, and coherent scattering for obtaining a measure of structure. Measurements of these parameters were made using a laboratory experimental set-up comprising an X-ray tube and HPGe detector. The investigated breast tissue samples comprised five different tissue classifications: adipose, malignant, fibroadenomatous, normal fibrous tissue, and tissue that had undergone fibrocystic changes. The coherent scattering spectra were analyzed using a peak fitting routine [11].

While the Monte Carlo (MC) codes are the best option for radiation simulation, there is one permanent defect with these codes and it is the lack of sufficient physical model for coherent (Rayleigh) scattering including molecular interference effects. Therefore, Tartari et al. proposed that the usual tabulations of coherent scattering data performed in the frame of independent atomic modelling (IAM) should be updated and replaced with molecular and intramolecular form factors related to each tissue or material. They obtained interference functions for fatty and bone tissues in terms of their mineral and nonmineral components [12]. Chaparian et al. also obtained interference functions for water and breast tissues [13].

In another study conducted by Chaparian et al., a system of EDXRD was optimized. In that study, the association between various setup parameters and some performance specifications such as sensitivity, spatial resolution, and momentum transfer resolution were assessed using both geometrical calculations and modeling. Accuracy of the derived associations was also confirmed by means of experimental measurements on water samples. Afterward the optimum parameters were determined for obtaining X-ray diffraction patterns from biological tissues for an efficient acquisition time. Finally, considering optimum parameters, the required measurement time for obtaining X-ray diffraction patterns was found to be in order of 30-40 second. Therefore, in comparison with other studies that required time between 400 and 600 seconds, they could considerably increase system sensitivity [1].

The aim of this study was to implement optimized setup and methods which were used in our previous studies [1, 13] and prove the success of this optimization. This was demonstrated by measuring the X-ray diffraction patterns of some tissue equivalent materials (acrylic, polyethylene, nylon, and calcium carbonate) and biological tissues (adipose, muscle, and bone).

2. Materials and Methods

2.1. Overview of the desired EDXRD setup

In the present study, a setup plan including an X-ray tube, two primary collimator diaphragms, two circular scatter collimator diaphragms, and a semiconductor detector (HPGe) was used (Figure 1).

The used source was a tungsten target conventional X-ray tube (model NGO) which could continuously operate at 50 kVp and 10 mA and its output was 8.26 mR/mA. The detector used in this study was a high purity germanium detector (model GPD 50/400 Ortec) with a cylindrical crystal of diameter 50 mm and thickness of 15 mm. This detector had an energy resolution of 0.49 keV at 59.5 keV.

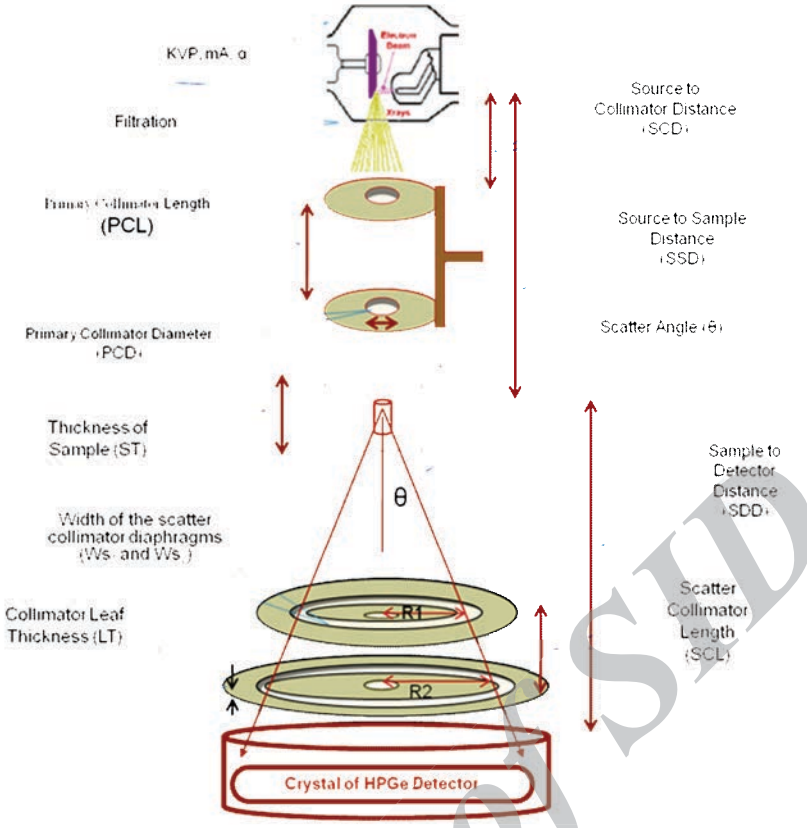

Figure 1. Schematic setup of EDXRD system applied in this study.

The distance between the two planes of the primary collimator specifies the primary collimator length (PCL) and the diameter of the holes specifies the primary collimator diameter (PCD). The width of the beam emerging from this collimator specifies the horizontal dimension of the region of interest (HROI). The primary collimator defines an X-ray pencil beam incident on the tissue sample. The photons scattered under a predefined scatter angle are collected by means of a rotationally symmetric scatter collimator consisting of two ring diaphragms with different diameters. The scatter angle (θ) can be set by moving the upper diaphragm of the collimator in the vertical direction or by changing the radius of the diaphragms. The main parameters of the scatter collimator are the width of the upper diaphragm (Ws1), width of the lower diaphragm (Ws2), radius of the upper diaphragm (R1), radius of the lower diaphragm (R2), the scatter collimator length (SCL), leaf thickness of the collimator (LT), sample to detector distance (SDD), and scatter angle (θ) (Figure 1).

2.2. Designing and building collimators and sample holder

A flexible tool constituting primary and scatter collimators and a sample holder were designed and built. This tool includes a special frame and five square holders which easily move relative to each other so that the distance between them is adjustable and each sheet of collimators is easily placed in the tool (Figure 2).

The primary collimator included two square lead sheets with side size of 115 mm which a hole with certain diameter was created in the center of them. Holes had different diameters, i.e., 0.5, 1, 2, 3, 4, and 5 mm. The scatter collimator also included two square lead sheets with side size of 115 mm which a circular groove with certain radius and width was created in the center of them. The circular grooves had different radiuses, i.e., 5, 8, 12, 15, and 18 mm which each certain radius had different widths, i.e., 0.5, 1, and 2 mm.

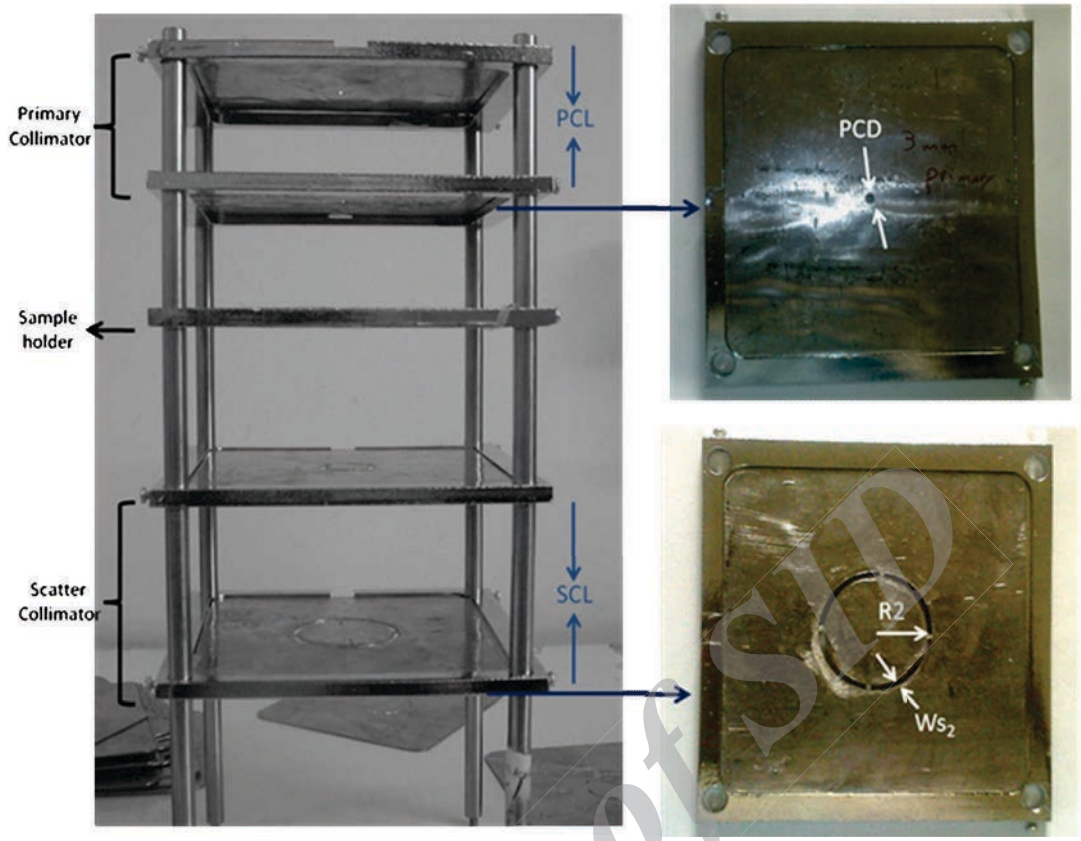

Figure 2. Illustration of designed tool constituting primary and scatter collimators and a sample holder.

The primary collimator sheets, the examined tissue sample, and the scatter collimator sheets were located on the frame from top to the bottom, respectively. During the experiment, the exit beam from X-ray tube which was shaped as a pencil beam by the primary collimator interacted with the tissue sample. The photons which scattered under a predefined scatter angle were allowed by the scatter collimator to get through and were recorded by the detector and the rest of the photons were absorbed.

2.3. Description of the measurements

During each measurement, after adjusting the collimators, the tissue sample was located on the sample holder (Figure 3). The exposure time of the X-ray tube and the recording time of the detector were adjusted. In order to increase the precision of the measurements, the time of exposure was started a little earlier than time of detection. The scattered radiation was analyzed using the HPGe detector for energy resolved photon detection. After pulse processing, the corresponding pulses were transferred to a PC-based multi-channel analyzer (MCA) for processing. The information in the form of counts versus channel number represented a 'X-ray diffraction pattern' characterizing the tissue. For each of the investigated tissues, measurements were repeated three times.

The X-ray diffraction patterns of some tissue equivalent materials (acrylic, polyethylene, nylon, and calcium carbonate) and biological tissues (adipose, muscle, and bone) were obtained.

The background spectrum was also measured with the same setup and time duration in the absence of the samples. The background spectrum was subtracted from each of the measured X-ray diffraction pattern. Since the EDXRD system is based on using a polyenergetic photon spectrum and intensity is different in each energy bin, the incident spectrum should be measured. In order to avoid paralysis of the detector due to high intensity of output, the primary beam was narrowed down using four primary collimator sheets.

Figure 3. The picture of measurement setup including X-ray tube, collimators and a semiconductor detector (HPGe).

2.4. Extraction of spectrum information

Spectra obtained from measurements were saved in form of ".spa" files in a computer connected to the detector. In order to display these patterns in other computers they should be converted to MATLAB files using related software and counting data were displayed by an appropriate software. It was necessary to correct the raw spectrum for several effects, i.e., background radiation, the non-uniform intensity spectrum of the incident beam, multiple scatter, and the attenuation of primary and scatter radiation. When the sample is relatively small, only the first two corrections are important. Therefore, after subtracting the background spectrum, the X-ray diffraction patterns were normalized to the intensity of the incident beam. It was also necessary to reduce fluctuations of the X-ray diffraction patterns using a curve fitting software.

3. Results

Figure 4 shows the measured X-ray diffraction patterns for tissue equivalent materials, i.e., acrylic (PMMA), polyethylene, nylon, and calcium carbonate. Figure 5 shows the measured X-ray diffraction patterns for biological tissues include adipose, muscle, and bone. Table 1 shows peak position of X-ray diffraction patterns for the examined tissue equivalent materials and biological tissues.

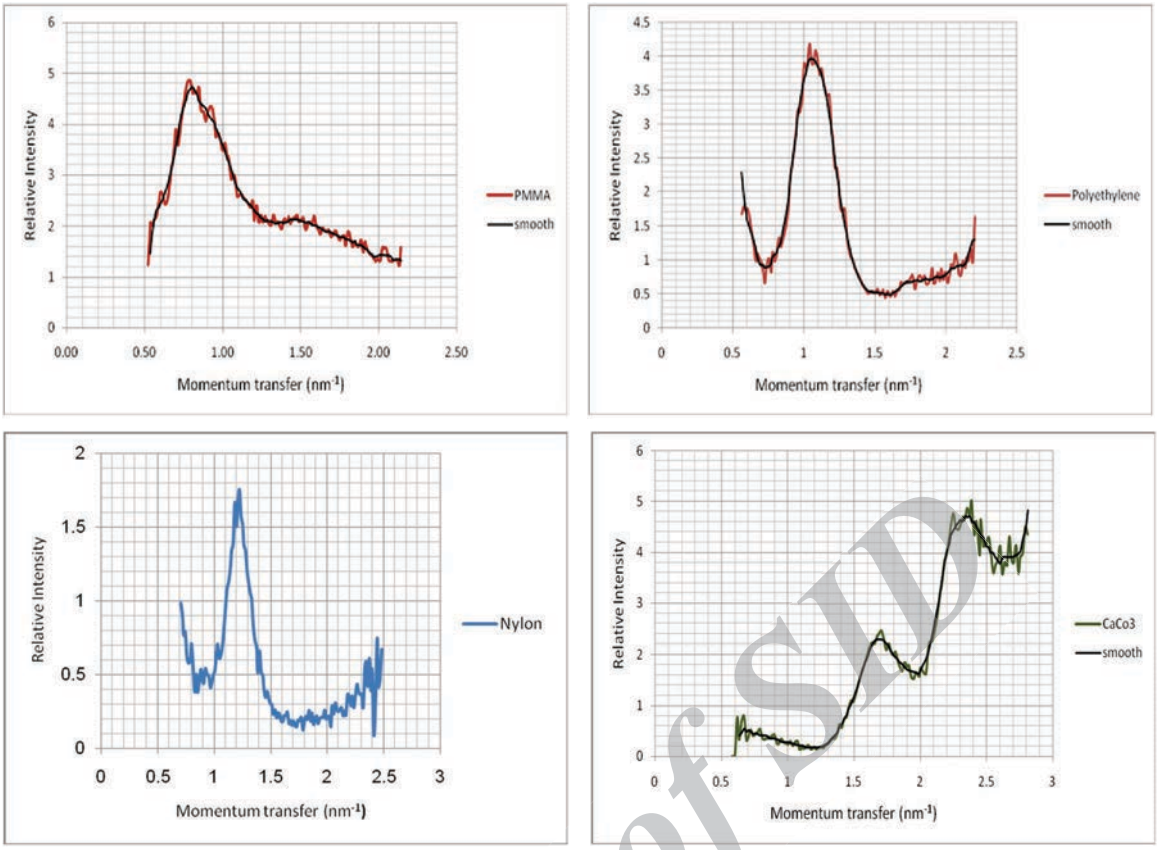

Figure 4. Diffraction patterns for a) acrylic (PMMA), b) polyethylene, c) nylon, and d) calcium carbonate.

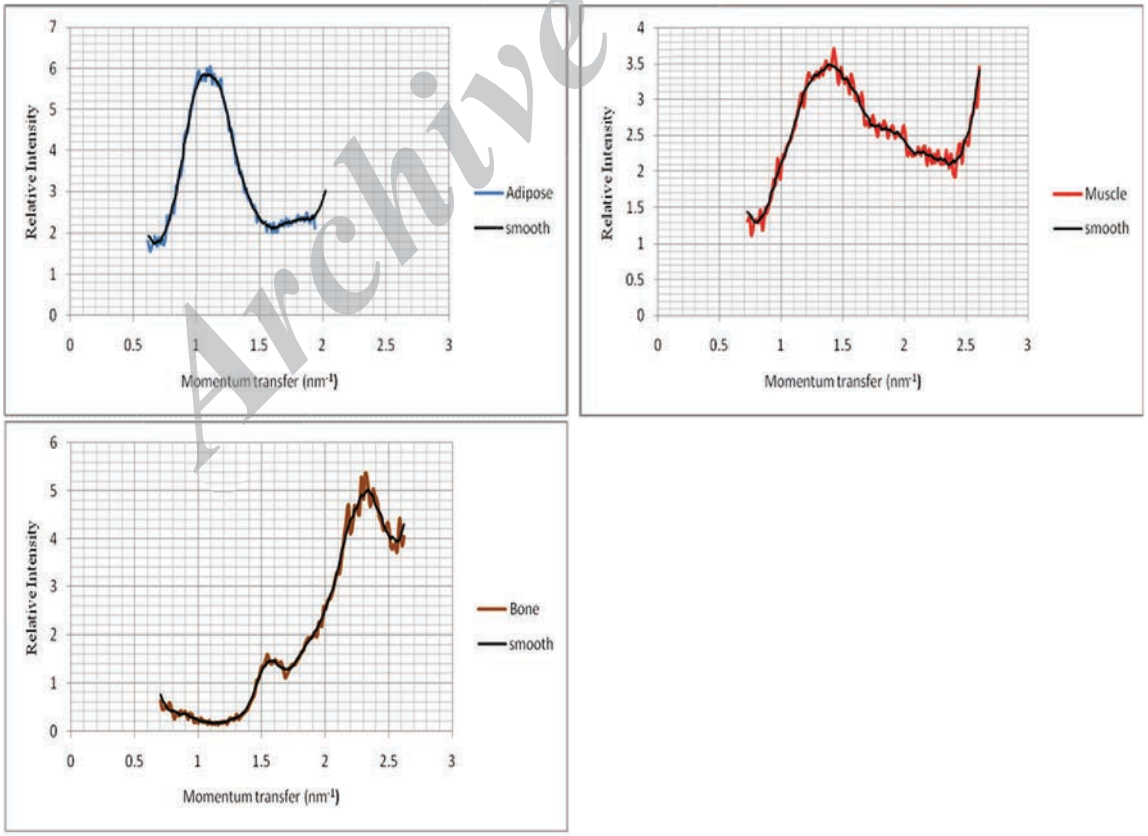

Figure 5. Diffraction patterns for a) adipose b) muscle and c) bone.

Table 1. The peak positions of X-ray diffraction patterns for some tissue equivalent materials and biological tissues.

Sample	Peak Positions (nm^{-1})
Acrylic (PMMA)	0.8±0.04
Polyethylene	1.03±0.051
Nylon	1.22±0.061
Calcium carbonate	1.7±0.085 & 2.3±0.115
Adipose	1.1±0.055
Muscle	1.41±0.072
Bone	1.6±0.08 & 2.3±0.115

4. Discussion

Results of this study proved efficacy of the system which was designed and optimized in our previous studies by obtaining the X-ray diffraction patterns for some tissue equivalent materials and biological tissues. The measured X-ray diffraction patterns of biological tissues were only offered for showing the efficacy of the designed system in differentiation of different tissues. Obviously, coherent investigation of any type of tissue required sufficient number of samples that was outside the scope of this study. The X-ray diffraction patterns obtained in this study were in good agreement with previous measurements in terms of peak position, but differences were observed in peak height. Disparities can be partially accounted for by the differences in the implemented setup.

As shown in Figure 4 (a-c), the peak positions for the acrylic, polyethylene, and nylon were found to occur at momentum transfer (x) values of 0.8±0.04 nm^{-1}, 1.03±0.051 nm^{-1}, and 1.22±0.061 nm^{-1}, respectively. As shown in figure 4 (d) the first and second peak positions for calcium carbonate were found to occur at momentum transfer (x) values of 1.7±0.085 nm^{-1} and 2.3±0.115 nm^{-1}, respectively. These results were similar to the X-ray diffraction patterns measured by Poletti et al [4, 7].

As shown in Figure 5 (a), the first peak position for adipose was found to occur at momentum transfer (x) value of 1.1±0.055 nm^{-1} which was similar to the X-ray diffraction patterns measured by other authors [6-9]. In addition, according to Figure 5 (b), the first peak position for the muscle was found to occur at momentum transfer (x) value of 1.41±0.072 nm^{-1} which partially agreed with the patterns obtained by Batchelar Deidre et al [3]. Also as shown in Figure 5 (c) the correspond the first and second peak positions of bone were found to occur at momentum transfer (x) values of 1.6±0.08 nm^{-1} and 2.3±0.115 nm^{-1}, respectively which had relative agreement with the patterns obtained by Speller et al [5].

As mentioned before, the EDXRD system is based on using a polyenergetic photon spectrum and intensity in each energy bin was different thus the X-ray diffraction patterns should be normalized to the intensity of the X-ray beam. The correction for the X-ray spectrum shape has the effect of increasing noise at low and high energies because of the poor statistical quality of the data. Therefore, an energy cut-off was applied below and above the useful range of momentum transfer values. This correction was also performed in the literature. For example, Kidane and colleagues [6] applied an energy cut-off below momentum transfer values of 0.70 nm^{-1} and above 3.26 nm^{-1}. The X-ray diffraction patterns of water measured by Leclair et al. had also applied this correction from momentum transfer of 0.6 nm^{-1} to 2.5 nm^{-1}. Slight differences can be partially accounted for by the difference in the applied setup, X-ray tube, and detector.

5. Conclusion

The results of this study showed that the X-ray diffraction patterns of any tissue could be extracted by our designed setup. This setup can be used as a supplement for routine clinical diagnostic methods. In mammography when distinguishing normal from cancerous mass is impossible, comparing simultaneously measured X-ray diffraction patterns is helpful.

Acknowledgment

We are grateful to Prof. M.J. Farquharson for suggestions regarding this work. This study was supported by Shahid Sadoughi University of Medical Sciences and Tehran University of Medical Sciences.

References

1. Chaparian A, Oghabian MA, Changizi V, Farquharson MJ. The optimization of an energy dispersive x-ray diffraction system for potential clinical application. Appl Radiat Isot. 2010 Dec;68(12):2237-45.
2. LeClair RJ, Boileau MM, Wang Y. A semianalytic model to extract differential linear scattering coefficient of breast tissue from energy dispersive x-ray diffraction measurements. Med Phys. 2006 Apr;33(4):959-67.
3. Batchelar DL, Davidson MT, Dabrowski W, Cunningham IA. Bone-composition imaging using Coherent-scatter computed tomography: Assessing bone health beyond bone mineral density. Med Phys. 2006 Apr;33(4):904-15.
4. Davidson MT, Batchelar DL, Chew BH, Denstedt JD, Cunningham IA. Establishing Composition and Structure of Intact Urinary Calculi by X-Ray Coherent Scatter for Clinical Laboratory Investigations. J Urol. 2006 Jun;175(6):2336-40.
5. Royle GJ, Speller RD. Quantitative X-ray diffraction analysis of bone and marrow volumes in excised femoral head samples. Phys Med Biol. 1995 Sep;40(9):1487-98.
6. Kidane G, Speller RD, Royle GJ, Hanby AM. X-ray scatter signatures for normal and neoplastic breast tissues. Phys Med Biol. 1999 Jul;44(7):1791-802.
7. Poletti ME, Gonçalves D, Mazzaro I. X-ray scattering from human breast tissues and breast-equivalent materials. Phys Med Biol. 2002 Jan 7;47(1):47-63.
8. Changizi V, Oghabian MA, Speller R, Sarkar S, Kheradmand AA. Application of small angle x-ray scattering (SAXS) for differentiation between normal and cancerous breast tissue. Int J Med Sci. 2005;2(3):118-21. Epub 2005 Jul 5.
9. Changizi V, Kheradmand AA, Oghabian MA. Application of small angle x-ray scattering (SAXS) for differentiation among breast tumors. J Med Phys. 2008 Jan;33(1):19-23.
10. Narten AH. X-ray diffraction data on liquid water in the temperature range 4 °C–200 °C. ORNL 1970 Report No. 4578.
11. Theodorakou C, Farquharson MJ. Human soft tissue analysis using x-ray or gamma-ray techniques Phys Med Biol. 2008 Jun 7;53(11):R111-49. Epub 2008 May 1.
12. Tartari A, Taibi A, Bonifazz C, Baraldi C. Updating of form factor tabulations for Coherent scattering of photons in tissues. Phys Med Biol. 2002 Jan 7;47(1):163-75.
13. Chaparian A, Oghabian MA, Changizi V. Acquiring molecular interference functions of X-ray Coherent scattering for breast tissues by combination of simulation and experimental methods. Iran J Radiat Res. 2009;7(2):113-7.